

Ultrafast photocarrier dynamics of black phosphorus under pressure

Hanyu Wang(王瀚宇), Shujuan Xu(许淑娟), Xinyao Wang(汪心瑶), Kai Zhang (张凯), Liangjiang Zou(邹良剑), and Fuhai Su(苏付海)

Citation: Chin. Phys. B, 2026, 35 (**5**): 056301. DOI: 10.1088/1674-1056/ae4b2e
http://cpb.iphy.ac.cn; http://iopscience.iop.org/cpb

What follows is a list of articles you may be interested in

New structures and properties of YF_3 and YF_6 under high pressure

Lebin Chang(常乐斌), Jianlun Huang(黄健伦), Yuhao Fu(付钰豪), Yingying Wang(王莹莹), and Jurong Zhang(张车荣)

Chin. Phys. B, 2026, 35 (**3**): 036301. DOI: 10.1088/1674-1056/ae1f02

Structure and properties of MgO melt at high pressure: A first-principles study

Min Wu(吴旻) and Zhongsen Sun(孙忠森)

Chin. Phys. B, 2025, 34 (**8**): 086301. DOI: 10.1088/1674-1056/add4e2

First-principles study on stability and superconductivity of ternary hydride $LaYH_x$ (x =2, 3, 6 and 8)

Xiao-Zhen Yan(颜小珍), Xing-Zi Zhou(周幸姿), Chao-Fei Liu(刘超飞), Yin-Li Xu(徐寅力), Yi-Bin Huang(黄毅斌), Xiao-Wei Sheng(盛晓伟), and Yang-Mei Chen(陈杨梅)

Chin. Phys. B, 2024, 33 (**8**): 086301. DOI: 10.1088/1674-1056/ad41b8

New carbon-nitrogen-oxygen compounds as high energy density materials

Junyu Shen(沈俊宇), Qingzhuo Duan(段青卓), Junyi Miao(苗俊一), Shi He(何适),Kaihua He(何开华), Wei Dai(戴伟), and Cheng Lu(卢成)

Chin. Phys. B, 2023, 32 (**9**): 096302. DOI: 10.1088/1674-1056/acce94

Thermal transport in semiconductor nanostructures, graphene, and related two-dimensional materials

Alexandr I. Cocemasov, Calina I. Isacova, Denis L. Nika

Chin. Phys. B, 2018, 27 (**5**): 056301. DOI: 10.1088/1674-1056/27/5/056301

SPECIAL TOPIC — Structures and properties of materials under high pressure

Ultrafast photocarrier dynamics of black phosphorus under pressure

Hanyu Wang(王瀚宇)[1,2,†], Shujuan Xu(许淑娟)[1,2,†], Xinyao Wang(汪心瑶)[1,2], Kai Zhang (张凯)[3], Liangjian Zou(邹良剑)[1], and Fuhai Su(苏付海)[1,‡]

[1] *Key Laboratory of Materials Physics, Institute of Solid State Physics, HFIPS, Chinese Academy of Sciences, Hefei* 230031, *China*
[2] *University of Science and Technology of China, Hefei* 230026, *China*
[3] *GBA Branch of Aerospace Information Research Institute, Chinese Academy of Sciences, Guangzhou* 510700, *China*

(Received 19 January 2026; revised manuscript received 12 February 2026; accepted manuscript online 27 February 2026)

In situ ultrafast photocarrier dynamics of multilayer black phosphorus (BP) are investigated under pressure using optical pump-probe spectroscopy. Below 10 GPa, the transient reflectivity exhibits sub-picosecond saturable absorption (SA) followed by oscillations arising from longitudinal coherent acoustic phonons (CAPs). With increasing pressure, pronounced anomalies in carrier relaxation and CAP behavior are observed, including a strong enhancement of CAP amplitude around 2.0 GPa, associated with a pressure-induced Lifshitz transition. Above 10 GPa the ultrafast response switches from SA to absorption enhancement (AE), accompanied by the complete disappearance of CAPs, indicating the transition to a cubic metallic phase. The pressure-dependent behavior of the CAPs reflects an enhanced interlayer coupling along the cross-plane direction, while the transition from SA to AE dynamics signifies a fundamental shift in in-plane carrier transport. Meanwhile, first-principles calculations reveal a pressure-induced reconstruction of the electronic structure and an increase in the longitudinal acoustic phonon group velocity across Lifshitz transition, supporting the microscopic understanding for anomalous CAP dynamics based on enhanced deformation-potential coupling and electron temperature of Dirac carriers. The study provides critical insights into the pressure-tuned topological transitions and the role of Dirac fermions in the nonequilibrium dynamics of compressed BP.

Keywords: black phosphorus, high pressure, ultrafast spectroscopy, Lifshitz transition, coherent acoustic phonons

PACS: 63.22.–m, 07.35.+k, 78.47.J–, 78.20.–e, 78.30.Am

DOI: 10.1088/1674-1056/ae4b2e **CSTR:** 32038.14.CPB.ae4b2e

1. Introduction

Black phosphorus (BP), a prototypical two-dimensional (2D) semiconductor, exhibits remarkable in-plane anisotropy in its electrical transport,[1–3] optical response,[4–6] thermal properties,[7,8] and electron-phonon interactions.[9] Under ambient pressure, orthorhombic BP (A17-phase) consists of puckered honeycomb layers stacked via van der Waals interactions along the *c*-axis. This unique atomic arrangement leads to a highly anisotropic electronic structure, where the energy dispersion is nearly linear along the armchair direction but parabolic along the zig-zag direction.[10] The band gap of BP is primarily governed by the out-of-plane p_z-like orbitals, making it highly sensitive to variations in interlayer coupling. Two primary mechanical strategies are typically employed to engineer the band gap of BP by manipulating its interlayer interactions: (i) thickness reduction via exfoliation to the monolayer limit (phosphorene), which decouples layers and expands the band gap from 0.3 eV (bulk) to approximately 2.0 eV;[11] and (ii) exerting hydrostatic pressure, which effectively reduces the band gap by modifying the height of the puckered layers and strengthening interlayer interactions. Upon compression, BP sequentially undergoes phase transitions from the A17-phase to the rhombohedral structure (A7 phase) at 5 GPa, and subsequently to a cubic metallic phase at 10 GPa.[12–15]

Beyond structural transitions, the electronic topology of BP evolves significantly under pressure. A notable example is the Lifshitz transition,[16,17] a change in the Fermi surface topology, which is proposed to occur around 1.5 GPa.[18] While Lifshitz transitions play a pivotal role in the transport properties of strongly correlated systems, their direct observation under high pressure remains an experimental challenge.[19] In BP, anomalies in electrical resistance and infrared absorption have been linked to this transition.[20,21] However, these equilibrium measurements are often susceptible to external factors such as doping and defects.[22] Ultrafast photoexcitation offers a powerful alternative by probing nonequilibrium carrier distributions and relaxation pathways dictated by carrier-carrier and carrier-phonon interactions.[23,24] Recently, the evolution of coherent phonons across structural phases in BP has been explored using ultrafast microscopy, revealing anomalous softening of shear modes within 3–8 GPa.[25] However, the behavior of longi-

[†] These authors contributed equally to this work.
[‡] Corresponding author. E-mail: fhsu@issp.ac.cn

© 2026 Chinese Physical Society and IOP Publishing Ltd. All rights, including for text and data mining, AI training, and similar technologies, are reserved.

tudinal coherent acoustic phonons (CAPs) and their specific response to the electronic Lifshitz transition remains largely unexplored.

In this work, we utilize high-pressure optical pump-probe spectroscopy (OPPS) to investigate the reflectivity transients of BP single crystals up to 11 GPa. We identify the pressure-induced Lifshitz transition as the central mechanism governing the evolution of nonequilibrium carrier and lattice dynamics, while structural phase transitions at higher pressures serve primarily as reference points to delineate distinct dynamical regimes. By combining ultrafast spectroscopy with density functional theory (DFT), we demonstrate that pronounced anomalies in photocarrier relaxation and CAP amplitudes emerge across the Lifshitz transition. These findings reveal the crucial role of Dirac fermions and enhanced electron-phonon coupling in shaping the ultrafast response of compressed BP.

2. Experimental details

BP single crystals synthesized by the high-pressure Bridgman method were purchased from a commercial supplier (2D Semiconductors). High pressure was generated using a diamond anvil cell (DAC). The diamond culet and the hole diameter of the stainless-steel gasket were 500 μm and 300 μm, respectively. Silicone oil was employed as the pressure-transmitting medium, and pressure calibration was carried out using the ruby fluorescence method by monitoring the R1 luminescence peak. To minimize sample degradation, the loading of the BP sample, pressure medium, and ruby sphere was performed inside a glove box equipped with an optical microscope. The BP single crystal was mechanically exfoliated into a thin platelet with a smooth and shiny surface. The typical lateral size of the sample was about 100×140 μm, with a thickness of approximately 5 μm along the c-axis. For optical measurements, the sample was arranged in a flat configuration and placed in direct contact with one diamond surface.

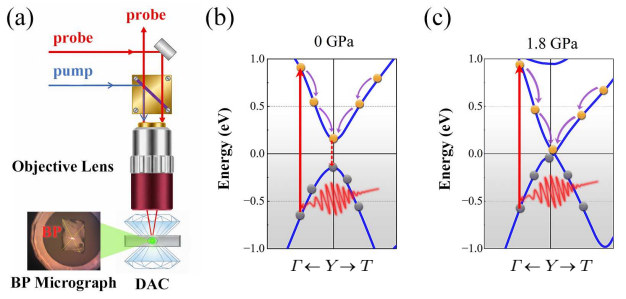


Fig. 1. (a) Schematic of the OPPS setup and optical micrograph of the BP sample inside the DAC. (b) and (c) Calculated energy band structures and diagrams of photocarrier dynamics at (b) 0 GPa and (c) 1.8 GPa.

OPPS experiments were performed using a Ti:sapphire femtosecond laser (Mira F900, Coherent) with a repetition rate of 76 MHz and a pulse duration of 150 fs. Both pump and probe pulses were tuned to the same central wavelength of 800 nm. The cross-polarized pump (s-polarized) and probe (p-polarized) beams were spatially separated by a polarizing beam splitter (PBS) cube and subsequently focused onto the sample inside the DAC by an objective lens, as shown in Fig. 1(a), with spot sizes of approximately 8 μm and 4 μm, respectively. The reflected probe beam passed through the PBS again, effectively suppressing scattered light from the orthogonally polarized pump beam. The reflected probe signal was detected using a biased silicon photodetector in conjunction with an RF lock-in amplifier. The pump beam was modulated by an acousto-optic modulator at a frequency of 1 MHz. The fluence ratio between the pump and probe beams was maintained at approximately 5:1. The pump fluence incident on the DAC was about 20 μJ/cm^2 below 10 GPa and 10 μJ/cm^2 above 10 GPa. All measurements were carried out at room temperature.

3. Results and discussions

We first performed first-principles calculations based on density functional theory (DFT), employing full geometry optimizations across a range of hydrostatic pressures up to 2 GPa. Detailed electronic structures under pressure are provided in Fig. S1 in Supplementary Material. At each pressure increment, both the lattice parameters and internal atomic coordinates were fully relaxed until the residual forces and stress tensors met the convergence criteria. Our results show that at ambient pressure, bulk BP exhibits a direct band gap of 0.28 eV (Fig. 1(b)). As the applied pressure increases, this band gap gradually narrows and eventually closes at approximately 1.8 GPa (Fig. 1(c)), marking the occurrence of a Lifshitz transition. After obtaining the band structures of BP, we performed OPPS to investigate the ultrafast photocarrier dynamics associated with interband and intraband transitions under various pressures. In Figs. 2(a) and 2(b), we present the differential reflectivity (DR) signals, which are defined as

$$\Delta R/R_0 = (R - R_0)/R_0 \tag{1}$$

as a function of the pump-probe delay within the initial 80 ps time window under several representative pressures, where R and R_0 denote the reflectivity with and without pump excitation, respectively. For clarity, the DR traces are vertically offset, with the baseline of each trace set to zero along the y-axis. At pressures below 9.6 GPa, the DR signal exhibits an initial fast negative dip followed by a long-lived periodic oscillation. During the measurement, the sample orientation was initially adjusted to achieve the longest oscillation damping time, indicating that the probe beam polarization was indeed parallel to the zigzag direction.[19] The photocarrier dynamics observed at 0.4 GPa are in good agreement with previously reported results for few-layer BP under ambient conditions.[26] The initial negative dip is indicative of nonlinear carrier dynamics arising

from saturable absorption (SA), where the probe absorption is reduced due to phase-space filling by photocarriers injected by the pump pulse.[27] The superimposed oscillatory component in the DR transients can be attributed to the excitation of longitudinal CAPs. Absorption of the pump pulse launches a CAP wave packet (or strain pulse) at the sample surface via thermoelastic or photoelastic effects, which subsequently propagates into the sample along the c-axis. The propagating CAP periodically modulates the local dielectric constant, giving rise to partial reflection of the probe pulse inside the sample. Consequently, constructive and destructive interference between probe photons reflected from the surface and the interior leads to the observed oscillatory DR signal.[28] As the pressure increases within the A17-phase (below 5 GPa), both the SA-induced negative dip and the CAP oscillations become more pronounced. In contrast, when the pressure exceeds 5 GPa, the DR signal is significantly suppressed as BP undergoes a structural transition into the A7 phase. Meanwhile, a positive DR component with a long decay time emerges, suggesting an enhanced photoconductivity response. Upon further compression above 9 GPa, BP is driven into the cubic phase, resulting in a complete reversal of the DR signal to a positive sign and a total disappearance of CAP-related oscillations. In the cubic phase, the DR transient is characterized by a rapid initial rise followed by a long decay, which can be well described by a biexponential fitting function. The absorption enhancement in the cubic phase is characteristic of photoinduced conductivity in a metallic system, dominated by intraband (Drude-like) carrier relaxation rather than phase-space filling.[29]

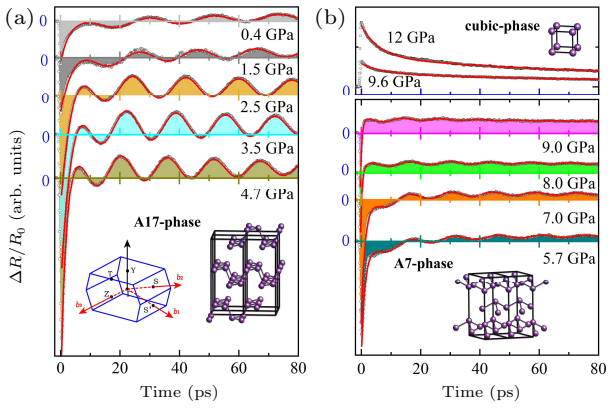


Fig. 2. The crystal structures, Brillouin zone, and differential reflectivity (DR) transients in the time domain measured under (a) the low-pressure region (below 5 GPa) and (b) the pressure range from 5 GPa to 12 GPa. For clarity, each DR trace is shifted vertically, whose baseline is denoted as zero at the y-axis. The insets depict the lattice structure of BP in the corresponding pressure range.

As shown in Fig. 2, for pressures below 9 GPa, the relaxation dynamics can be quantitatively described by a damped harmonic oscillator model combined with a multiexponential decay function, a phenomenological approach widely adopted to describe coherent acoustic phonons and carrier relaxation processes[30,31]

$$\frac{\Delta R}{R_0} = A_1 \exp\left(-\frac{t}{\tau_1}\right) + A_2 \exp\left(-\frac{t}{\tau_2}\right) + B \exp\left(-\frac{t}{\tau_{\mathrm{CAP}}}\right) \cos(2\pi f_{\mathrm{CAP}} t - \varphi), \quad (2)$$

where B is the CAP amplitude, f_{CAP} is the CAP frequency, τ_{CAP} is the lifetime of CAP, and φ is the initial phase of CAP oscillations. A_1 and A_2 denote the amplitudes of the fast and slow decay components, respectively. τ_1 and τ_2 correspond to the time constants of the fast and slow decay, respectively. Correspondingly, the extracted time constants and CAP frequency are summarized in Fig. 3. The τ_1 and τ_2 can be attributed to the energy relaxation of hot carriers through electron–phonon (e–ph) scattering and subsequent interband recombination, respectively.[32] Notably, within the A17-phase, τ_1 initially increases with pressure, reaching a maximum around 2 GPa, then decreases. This turning point coincides with the critical pressure of the Lifshitz transition,[33] and that of band gap closure from our calculation. The Lifshitz transition-induced band inversion leads to a topological semimetallic state with one-dimensional (1D) or 2D Dirac cones.[34] We tentatively ascribe the pressure evolution of τ_1 to variations in the hot phonon bottleneck (HPB) effect across the Lifshitz transition. As illustrated in Figs. 1(b) and 1(c), above band gap photoexcitation injects electron–hole pairs with excess kinetic energy, which rapidly thermalize via electron-electron scattering within tens of femtoseconds, establishing a hot carrier distribution with an elevated electron temperature T_{e}. Subsequent energy relaxation to the lattice proceeds through e–ph interactions involving optical and acoustic phonons.[29] As the bandgap narrows with pressure, T_{e} is expected to rise, potentially enhancing hot phonon accumulation and strengthening the HPB effect, thereby prolonging τ_1. However, upon the emergence of Dirac dispersion via the Lifshitz transition, electron–electron scattering is anticipated to intensify significantly due to an enlarged phase space where both energy and momentum conservation can be simultaneously satisfied. This strong carrier-carrier scattering, combined with the small Fermi surface characteristic of Dirac systems, should further elevate T_{e}.[35] These factors suggest that the HPB effect alone cannot fully account for the observed reduction in τ_1. We propose that the higher T_{e} activates more frequent high-frequency optical phonon scattering, which suppresses the HPB effect and shortens τ_1. The pressure dependence of τ_2 also shows anomalies across the Lifshitz transition. Below 2 GPa, τ_2 decreases noticeably with pressure and becomes indistinguishable between 2 GPa and 5 GPa, consistent with bandgap closure. The abrupt changes in both τ_1 and τ_2 near 5 GPa are attributed to the structural transition from the A17 to the A7 phase, while anomalies in the 8–9 GPa range suggest the coexistence of A7 phase and cubic BP prior to full

conversion to the cubic structure. This interpretation is consistent with previous synchrotron XRD studies, which have demonstrated that the structural transition to the cubic phase in BP is a reconstructive process that typically exhibits a broad coexistence window.[36] Our results capture this transition as a progressive shift in the carrier dynamics rather than an instantaneous structural jump.

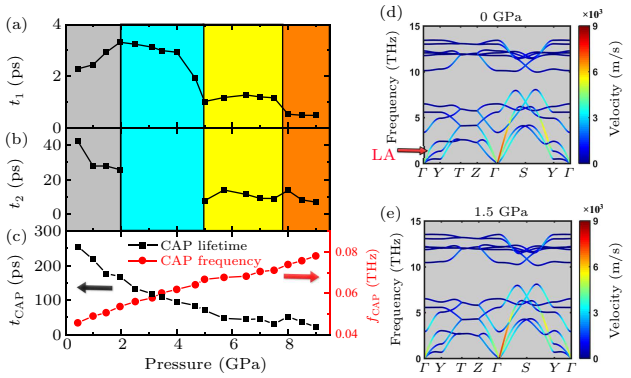


Fig. 3. Pressure-dependent carrier relaxation dynamics and phonon dispersion evolution. (a)–(b) Extracted time constants for carrier dynamics: (a) the fast decay component τ_1 and (b) the slow decay component τ_2 as a function of pressure. The shaded regions delineate different physical regimes, with the turning point near 2 GPa corresponding to the Lifshitz transition. (c) CAP parameters: evolution of the extracted CAP frequency f_{CAP} (red circles) and lifetime τ_{CAP} (black squares) with pressure. (d)–(e) Calculated phonon dispersion of BP at 0 GPa and 1.5 GPa, respectively, where the color gradient represents the group velocity v_g (m/s) of the phonon branches.

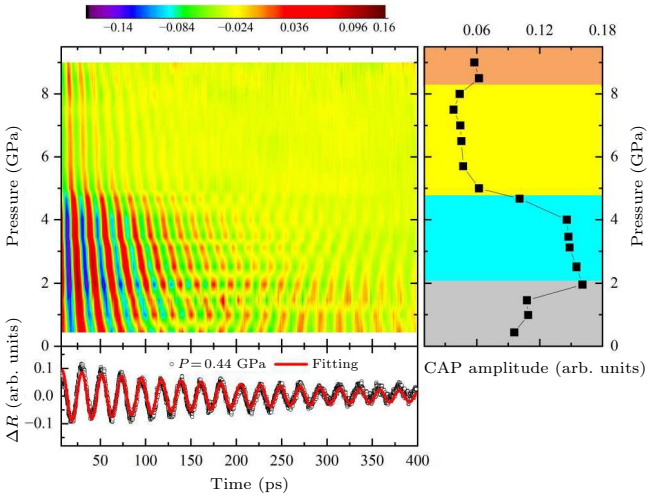


Fig. 4. Detailed analysis of CAPs. (Top left) 2D contour plot: differential reflectivity ($\Delta R/R_0$) transients as a function of delay time and pressure after subtracting the electronic relaxation background. (Bottom left) Representative fits: experimental data (circles) at 0.44 GPa, along with corresponding fits (red lines) using the damped harmonic oscillator model (Eq. (2)). (Right) CAP amplitude analysis: normalized CAP amplitude as a function of pressure. Shaded background colors distinguish A17 phase, A7 phase, and phase coexistence regions.

We now turn to the pressure dependence of the CAP oscillations. The extracted CAP frequency f_{CAP} and decay time τ_{CAP}, plotted as functions of pressure in Fig. 3(c). f_{CAP} increases monotonically with pressure, with a slight change in slope around the structural transition near 5 GPa. It is known that CAP oscillation is damped with frequency $f_{CAP} = 2nv_g/\lambda$ and decay time $\tau_{CAP} = \zeta/v_g$.[28] Here, v_g and n correspond to the sound group velocity and refractive index, respectively. λ and ζ denote the wavelength and optical absorption depth of probe light, respectively. The increased CAP frequency thus directly reflects the pressure-induced lattice stiffening and corresponding rise in sound velocity. To corroborate this interpretation, we performed first-principles calculations to obtain the phonon dispersions, shown in Figs. 3(d) and 4(e), with group velocities indicated by a color gradient. Our calculation indicates that the v_g of the longitudinal acoustic (LA) mode at the Γ point increases significantly from 4604.5 m/s at 0 GPa to 5301.9 m/s at 1.5 GPa. The observed blueshift in f_{CAP} is a direct consequence of lattice stiffening and enhanced interlayer coupling under compression. Correspondingly, τ_{CAP} decreases with pressure due to the increased sound velocity, shortening the propagation time across the optical absorption depth. It is important to note that neither f_{CAP} nor τ_{CAP} shows any discernible anomaly near 2 GPa, confirming that the lattice structure remains intact across the Lifshitz transition.

To further focus on the CAP, the color map of DR transients in the 15–400 ps time window at different pressures are shown in Fig. 4, with the electronic relaxation background subtracted. The CAP amplitude at each pressure is normalized to the negative peak of the electronic response to mitigate extrinsic effects from gasket deformation or pressure-medium absorption. A representative experimental trace under 0.44 GPa is plotted in the lower panel. A clear distinction emerges between the low-pressure A17 phase (strong CAP signal below 5 GPa) and the high-pressure A7 phase (weak signal above 5 GPa), underscoring 5 GPa as the critical pressure for the structural transition. The normalized CAP amplitude as a function of pressure is also shown in Fig. 4 (right panel). The prominent observation is that the CAP amplitude exhibits a sudden augmentation around 2 GPa, aside from the turning point at 4 GPa. We propose that the enhancement in CAP excitation is closely correlated with a Lifshitz transition. The CAP excitation in BP is generally considered to be dominated by the deformation potential mechanism.[19] In this case, the photo-induced stress σ that drives the CAP is proportional to the deformation potential constant Ξ. Here, the relation $\Xi = \partial E_n(k)/\partial\eta$ quantifies the sensitivity of the electronic energy levels $E_n(k)$ to lattice strain η.[37,38] Near the Lifshitz transition, the band-edge states involved in optical excitation exhibit a rapidly varying density of states (DOS) and enhanced band curvature sensitivity to strain, which effectively amplifies the deformation potential coupling, leading to a maximized deformation potential Ξ. In addition, the formation of Dirac electronic dispersion across the Lifshitz transition facilitates more efficient electron heating upon ultrafast photoexcitation, leading to a sudden elevation of electron temperature above 2 GPa as discussed above. Given that the photoinduced stress also scales linearly with electron temperature, we propose that the synergy between the increased T_e and the

enhanced Ξ (which strengthens electron-phonon coupling) results in the highly efficient generation of CAPs observed experimentally. This correlation underscores the pivotal role of the Lifshitz transition in modulating the nonequilibrium lattice dynamics of BP.

4. Conclusion

In summary, we have systematically investigated the pressure-dependent ultrafast photocarrier and CAP dynamics in multilayer BP up to 11 GPa. Our study reveals a complex interplay between structural phase transitions and topological electronic states:

(i) Spectroscopic Hallmarks of phase transitions: The transient reflectivity signals exhibit distinct regimes corresponding to BP's structural evolution. Below 10 GPa, the dynamics are dominated by sub-picosecond SA and robust CAP oscillations. Upon transitioning to the cubic metallic phase above 10 GPa, a dramatic reversal from SA to AE occurs, accompanied by the complete suppression of CAPs, marking the collapse of the layered anisotropic structure.

(ii) Signatures of the Lifshitz transition: A significant enhancement in both CAP frequency and amplitude is observed around 1.5 GPa. Combining experimental results with DFT calculations, we demonstrate that the frequency blueshift is driven by the stiffening of the lattice and the increase in the LA mode group velocity.

(iii) Deformation potential coupling: Based on deformation potential theory, the pronounced surge in CAP amplitude is attributed to the pressure-induced Lifshitz transition. The emergence of Dirac fermions and the topological reconfiguration of the Fermi surface significantly enhance the sensitivity of the energy bands to lattice strain, leading to a maximized deformation potential and intensified electron-phonon coupling.

Our findings highlight the power of high-pressure ultrafast spectroscopy in probing hidden topological transitions that are often elusive in equilibrium measurements. The discovery of enhanced CAP–Dirac fermion coupling opens new avenues for the coherent control of collective excitations in compressed 2D materials.

Acknowledgment

Project supported by the National Natural Science Foundation of China (Grant Nos. 12174398 and 12574466).

References

[1] Qiao J, Kong X, Hu Z X, Yang F and Ji W 2014 *Nat. Commun.* **5** 4475
[2] Fei R and Yang L 2014 *Nano Lett.* **14** 2884
[3] Kim J, Baik S S, Ryu S H, Sohn Y, Park S, Park B G, Denlinger J, Yi Y, Choi H J and Kim K S 2015 *Science* **349** 723
[4] Wang X, Jones A M, Seyler K L, Vy T, Jia Y, Zhao H, Wang H, Yang L, Xu X and Xia F 2015 *Nat. Nanotechnol.* **10** 517
[5] Xia F, Wang H and Jia Y 2014 *Nat. Commun.* **5** 4458
[6] Yuan H, Liu X, Afshinmanesh F, Li W, Xu G, Sun J, Lian B, Curto A G, Ye G, Hikita Y, Shen Z, Zhang S C, Chen X, Brongersma M, Hwang H Y and Cui Y 2015 *Nat. Nanotechnol.* **10** 707
[7] Luo Z, Maassen J, Deng Y, Du Y, Garrelts R P, Lundstrom M S, Ye P D and Xu X 2015 *Nat. Commun.* **6** 8572
[8] Zeng Q, Sun B, Du K, Zhao W, Yu P, Zhu C, Xia J, Chen Y, Cao X, Yan Q, Shen Z, Yu T, Long Y, Koh Y K and Liu Z 2019 *2D Mater.* **6** 045009
[9] Ling X, Huang S, Hasdeo E H, Liang L, Parkin W M, Tatsumi Y, Nugraha A R, Puretzky A A, Das P M, Sumpter B G, Geohegan D B, Kong J, Saito R, Drndic M, Meunier V and Dresselhaus M S 2016 *Nano Lett.* **16** 2260
[10] Kim J, Baik S S, Ryu S H, Sohn Y, Park S, Park B G, Denlinger J, Yi Y, Choi H J and Kim K S 2015 *Science* **349** 723
[11] Woomer A H, Farnsworth T W, Hu J, Wells R A, Donley C L and Warren S C 2015 *ACS Nano* **9** 8869
[12] Li X, Sun J, Shahi P, Gao M, MacDonald A H, Uwatoko Y, Xiang T, Goodenough J B and Cheng J 2018 *Proc. Natl. Acad. Sci. USA* **115** 9935
[13] Scelta D, Baldassarre A, Serrano-Ruiz M, Dziubek K, Cairns A B, Peruzzini M, Bini R and Ceppatelli M 2017 *Angew. Chem. Int. Ed.* **56** 14135
[14] Liu J, Zhang L, Wang Z, Zhao M, Wu B, Long H, Xue C, Tao Y, Du M, Wang Y, Wang Z and Li L 2025 *Appl. Phys. Lett.* **127** 213103
[15] Shen Y, Chen Z, Zhu Q, Huang Y and Pan W 2024 *Langmuir* **40** 24863
[16] Liu C, Kondo T, Fernandes R M, Palczewski A D, Mun E D, Ni N, Thaler A N, Bostwick A, Rotenberg E, Schmalian J, Bud'ko S L, Canfield P C and Kaminski A 2010 *Nature Phys* **6** 419
[17] Nishimura T, Sakai H, Mori H, Akiba K, Usui H, Ochi M, Kuroki K, Miyake A, Tokunaga M, Uwatoko Y, Katayama K, Murakawa H and Hanasaki N 2019 *Phys. Rev. Lett.* **122** 226601
[18] Zou L J, Sun Z, Zhang Y, Jiao L, Chen X H and Wen H H 2015 *Phys. Rev. Lett.* **115** 186403
[19] Meng S, Shi H, Jiang H, Sun X and Gao B 2019 *J. Phys. Chem. C* **123** 20051
[20] Li C H, Long Y J, Zhao L X, Shan L, Ren Z A, Zhao J Z, Weng H M, Dai X, Fang Z, Ren C and Chen G F 2017 *Phys. Rev. B* **95** 125417
[21] Di Pietro P, Mitrano M, Caramazza S, Capitani F, Lupi S, Postorino P, Ripanti F, Joseph B, Ehlen N, Grüneis A, Sanna A, Profeta G, Dore P and Perucchi A 2018 *Phys. Rev. B* **98** 165111
[22] Alkauskas A, McCluskey M D and Van de Walle C G 2016 *J. Appl. Phys.* **119** 181101
[23] Breusing M, Kuehn S, Winzer T, Malić E, Milde F, Severin N, Rabe J P, Ropers C, Knorr A and Elsaesser T 2011 *Phys. Rev. B* **83** 153410
[24] Tielrooij K J, Song J C W, Jensen S A, Centeno A, Pesquera A, Zurutuza Elorza A, Bonn M, Levitov L S and Koppens F H L 2013 *Nat. Phys.* **9** 248
[25] Wu S, Chu W, Lu Y and Ji M 2024 *Nano Lett.* **24** 424
[26] Miao X, Zhang G, Wang F, Yan H and Ji M 2018 *Nano Lett.* **18** 3053
[27] Wang K, Szydlowska B, Wang G, Zhang X, Wang J, Magan J, Zhang L, Coleman J, Wang J and Blau W 2016 *ACS Nano* **10** 6923
[28] Matsuda O, Larciprete M C, Li Voti R and Wright O B 2015 *Ultrasonics* **56** 3
[29] Sabbah A J and Riffe D M 2002 *Phys. Rev. B* **66** 165217
[30] Thomsen C, Strait J, Vardeny Z, Maris H J, Tauc J and Hauser J J 1986 *Phys. Rev. B* **34** 4129
[31] Hase M, Kitajima M, Nakashima S and Mizoguchi K 2002 *Phys. Rev. Lett.* **88** 067401
[32] Iyer V, Ye P and Xu X 2017 *2D Mater.* **4** 021032
[33] Xiang Z J, Ye G J, Shang C, Lei B, Wang N Z, Yang K S, Liu D Y, Meng F B, Luo X G, Zou L J, Sun Z, Zhang Y and Chen X H 2015 *Phys. Rev. Lett.* **115** 186403
[34] Fei R, Tran V and Yang L 2015 *Phys. Rev. B* **91** 195319
[35] Bistritzer R and MacDonald A H 2009 *Phys. Rev. Lett.* **102** 206410
[36] Joseph B, Caramazza S, Capitani F, Clarté T, Ripanti F, Lotti P, Lausi A, Castro D Di, Postorino P and Dore P 2018 *J. Phys.: Condens. Matter* **30** 494002
[37] Ruello P and Gusev V E 2015 *Ultrasonics* **56** 21
[38] Li Z, Graziosi P and Neophytou N 2021 *Phys. Rev. B* **104** 195201